Conf-941144--42
SAND94-1736C

RECIPROCAL SPACE ANALYSIS OF THE MICROSTRUCTURE OF LUMINESCENT AND NONLUMINESCENT POROUS SILICON FILMS

S.R. LEE, J.C. BARBOUR, J.W. MEDERNACH, J.O. STEVENSON AND J.S. CUSTER
Sandia National Laboratories, Albuquerque, NM 87185

ABSTRACT

The microstructure of anodically prepared porous silicon films was determined using a novel x-ray diffraction technique. This technique uses double-crystal diffractometry combined with position-sensitive x-ray detection to efficiently and quantitatively image the reciprocal space structure of crystalline materials. Reciprocal space analysis of newly prepared, as well as aged, p^- porous silicon films showed that these films exhibit a very broad range of crystallinity. This material appears to range in structure from a strained, single-crystal, sponge-like material exhibiting long-range coherency to isolated, dilated nanocrystals embedded in an amorphous matrix. Reciprocal space analysis of n^+ and p^+ porous silicon showed these materials are strained single-crystals with a spatially-correlated array of vertical pores. The vertical pores in these crystals may be surrounded by nanoporous or nanocrystalline domains as small as a few nm in size which produce diffuse diffraction indicating their presence. The photoluminescence of these films was examined using 488 nm Ar laser excitation in order to search for possible correlations between photoluminescent intensity and crystalline microstructure.

INTRODUCTION

The goals of this study were two-fold. The first was to assess the ability of a relatively new technique for reciprocal space analysis, based on position-sensitive x-ray detection, to yield new insights into the crystalline microstructure of various types of porous silicon. In order to do this, reciprocal space analysis was used to survey the microstructure of both newly prepared and aged porous silicon films anodized under a variety of conditions. Perhaps not surprisingly -- given the wide range of conclusions reached in transmission electron microscopy (TEM), transmission electron diffraction and x-ray diffraction studies that are already published -- the porous silicon studied here was found to exhibit a wide range of crystallinity and a diverse microstructure. Using reciprocal space analysis, we found that we could observe and quantify the following microstructural phenomena: nanocrystal and nanovoid size and shape, nanocrystal orientation, lattice dilation in films containing isolated nanocrystals, lattice strain distributions in films which remain single crystalline, and mean pore spacing in single-crystalline samples containing vertical pore arrays. Results for three prototypical porous silicon structures are presented in detail below in order to demonstrate the unique capabilities offered by reciprocal space analysis.

Quantitative determinations of the size, shape and volume-fraction of nanocrystalline domains that exist in various forms of porous silicon are of particular interest because of their relevance to quantum confinement as a mechanism for photoluminescence (PL) in porous silicon. Our second goal was to attempt to test the quantum confinement hypothesis by looking for the presence or absence of a quantitative correlation between relative PL efficiency and relative nanocrystal density. Thus, following structural characterization by reciprocal space analysis, photoluminescence measurements were made on all samples. While our comparisons of photoluminescence and microstructural results are not yet on a fully quantitative footing, an initial discussion of photoluminescence and microstructural results is presented.

DISCLAIMER

DISCLAIMER

Portions of this document may be illegible in electronic image products. Images are produced from the best available original document.

EXPERIMENTAL

(100)-oriented, 625 μm-thick Si wafers that were doped n^+, p^+ or p^- were anodized at constant current. The electrochemical cell was a bowl-type arrangement with a Au-plated metal platen contacting the Si backside to form an anode at the bottom of the cell. A Pt mesh was suspended above the Si as the cathode. A schematic of the cell appears in reference [1]. The samples for which we present detailed reciprocal space analysis results were anodized in (1:1) HF:ethanol. Additional specific details for the anodization of each sample are presented below.

Reciprocal space analysis of the porous Si was carried out using an apparatus that consists of a standard, double-crystal, x-ray diffractometer which has been modified by the addition of a position-sensitive x-ray detector (PSD) [2-4]. The PSD simultaneously measures the total scattering angle of diffracted x-rays emerging from the sample over a wide range of 2θ angles. This highly parallel analysis of the scattering angle allows one to map reciprocal space more than 100 times faster than can be done using a traditional, serially-scanned, triple-axis diffractometer. The tradeoff is a substantial decrease in resolution relative to that of a triple-axis system [4]. Reciprocal space maps were produced by measuring the diffracted x-ray intensity as a function of the rocking angle of the sample, ω, and the scattering angle, 2θ. Intensity as a function of angle, $I(\omega,2\theta)$, was then mapped into an intensity function in reciprocal space, I(K[00l],K[hh0]), using a coordinate transformation derived from an Ewald sphere construction [3].

The photoluminescent signal was excited by 488 nm wavelength light from a multi-mode Ar laser. The excitation light was incident at 45° from the sample normal, and the PL light was collected at an angle of 10° from the sample normal in an optical fiber. The illumination spot-size was ≈ 1 mm in diameter, and the power density was ≈ 1.5 W/cm^2. The emitted PL light was analyzed using a monochromator with a 150 groove/mm grating and detected with a thermoelectrically-cooled CCD photodetector. The resolution of this system was measured to be 2.3 nm over the range of wavelengths for the porous silicon light emission. Illumination times varied from 1-100 seconds depending on luminescent intensity.

RECIPROCAL SPACE ANALYSIS RESULTS

Figure 1 shows reciprocal space maps for (004) and (224) diffraction from a 0.78 Ω-cm, p-type sample, produced by anodization at 80 ma/cm^2 for 5 minutes. The sample is 20 μm thick and has a porosity of 69%. For this sample, diffraction and PL results were collected after the sample was stored in air for more than one year. The diffraction patterns of Figure 1 are consistent with a microstructure made of isolated nanocrystals dispersed in an amorphous matrix.

The intense center spot in Figures 1(a) & 1(b) is due to substrate diffraction. The extended diagonal streak in each figure is an artifact produced by reducing the diffractometer power as the scan rocks through the intense substrate peak. This is required in order to avoid damage to the PSD. This streak fortuitously marks the orientation of the Ewald sphere in each scan.

The important feature in Figure 1 is the diffuse pattern surrounding the substrate peak. This intensity consists of two components: thermal diffuse and background scattering from the substrate, and nanocrystal diffraction in the porous layer. The broadening of the diffuse intensity along K[hh0] in Figure 1(a), and its rotation between (004) and (224) so that it remains normal to an axis passing through the origin of reciprocal space, is consistent with the presence of nanocrystals that are slightly misoriented with respect to the substrate. The width along K[hh0] in Figure 1(a) indicates that the nanocrystals are tilted away from the substrate [001] axis by < 1.6°.

Figure 2 shows the same data as in Figure 1(a) minus the large background due to substrate scattering. This residual intensity is due only to nanocrystalline scattering in the porous layer.

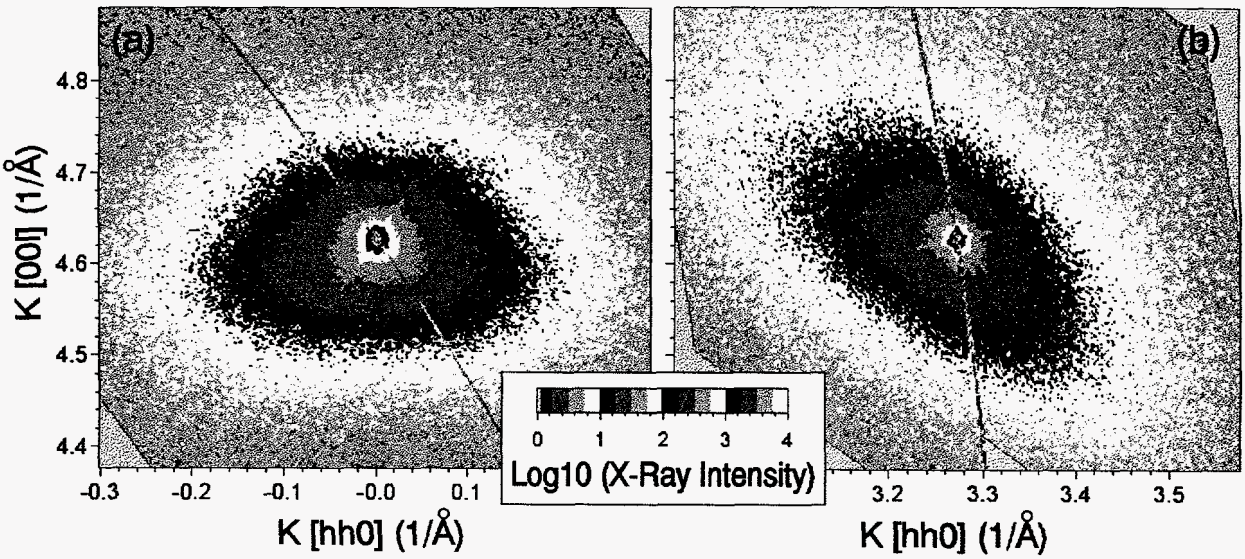

Figure 1. (a) the (004) diffraction pattern, and (b) the (224) diffraction pattern produced by p⁻ porous Si composed of isolated nanocrystals embedded in an amorphous matrix.

Using the width of this intensity peak along the K[00l] direction and the Scherrer particle size formula, or by direct comparison with reciprocal space simulations based on the kinematic theory of diffraction by small crystals [5], these nanocrystals are found to be 3-5 nm in diameter. Taking into account the broadening of the intensity distribution along K[hh0] due to misorientation effects, the reciprocal space intensity is approximately spherical. This indicates that on average these nanocrystals are spherical in shape. Finally, the vertical shift in the centroid of the peak to a K[00l] coordinate smaller than that of the substrate indicates that the nanocrystal lattice has dilated. The average nanocrystal perpendicular lattice constant is found to be 5.470 Å. Assuming a cubic dilation, based on similar asymmetries in the (004) and (224) diffuse scattering shown in Figure 1, a dilation of 0.72% is obtained. This agrees quite well with previous measurements where dilations of 0.65% [6] and 0.95% [7] were found for Si nanocrystals 4 nm in diameter.

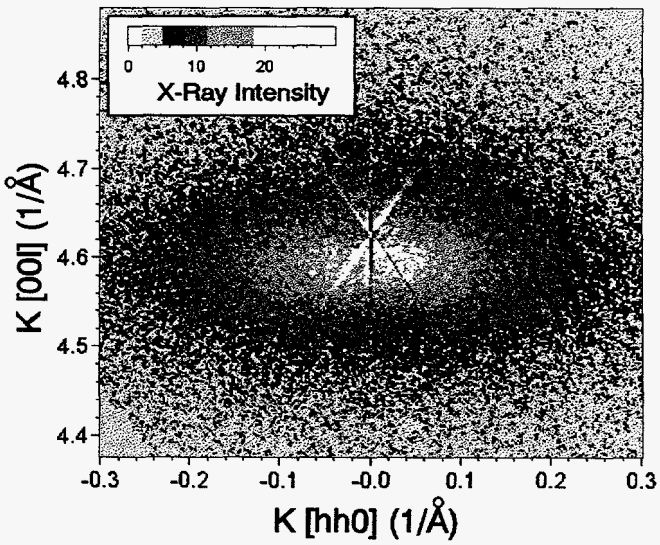

Figure 2. The (004) diffraction pattern produced by p⁻ porous Si, after subtraction of substrate background scattering, showing dilation of the nanocrystal lattice.

As a second example of reciprocal space analysis of porous silicon, figure 3 shows reciprocal space maps for (004) and (224) diffraction from a 0.86 Ω-cm, p-type sample, produced by anodization at 80 ma/cm^2 for 30 minutes. This sample is 120 μm thick and has a porosity greater than 69%. In this case, diffraction and PL results were collected after the sample was stored in air for about four days. At first glance, the intense diffuse scattering, the large width of the diffuse intensity along K[00l], and the rotation of the diffuse intensity on going from (004) to (224) again suggests nanocrystals that are a few nm in diameter. However, in

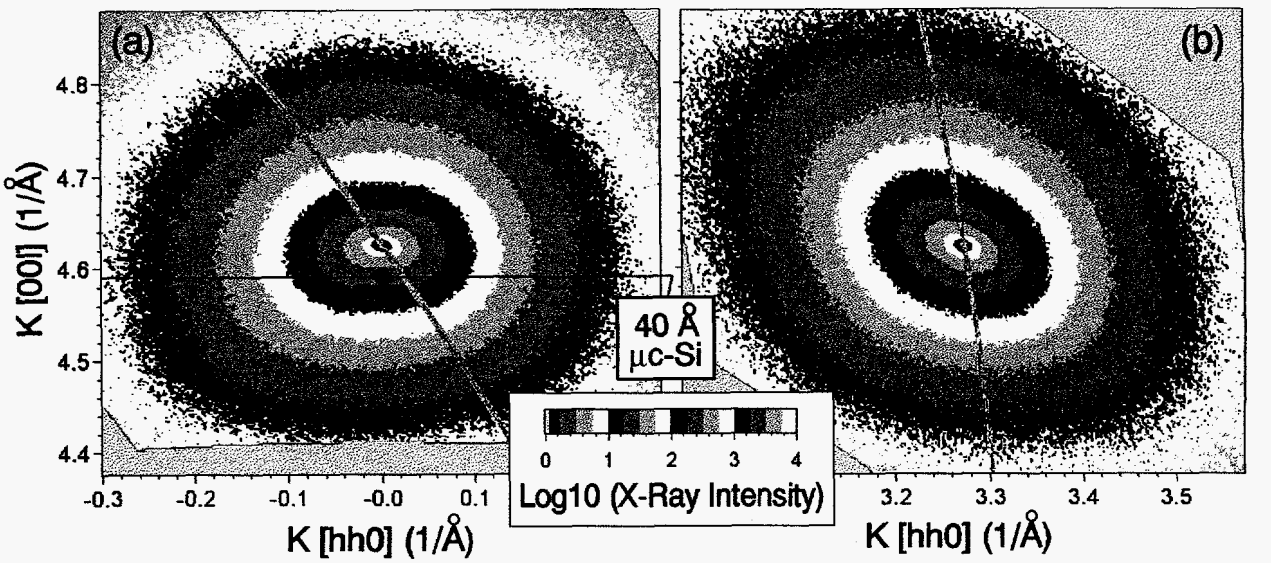

Figure 3. (a) the (004) diffraction pattern, and (b) the (224) diffraction pattern produced p^- porous Si composed of a single-crystal sponge and misoriented, sponge-like domains a few tens of nm in size.

Figure 3(a) we have marked the expected centroid position due to diffraction by dilated, 4-nm-diameter nanocrystals. The observed diffraction pattern is symmetrically centered about the Si substrate peak, and there is no distortion of the pattern in the direction of the expected dilation. This is inconsistent with a dilated, few-nm-diameter, nanocrystalline picture of microstructure.

In contrast to the aged p^- sample discussed above, combined (004) and (224) rocking curve results (not shown) reveal that a coherently strained, crystalline sponge comprises at least a portion of this anodized layer. The intensity of the layer's strain peak was weak (30x smaller than the substrate peak) despite the large thickness of the anodized layer. This may be because this coherently diffracting domain is a thin portion of the entire layer, or it may result from a thicker, but highly disordered layer that retains only partial coherency. This layer has a parallel lattice constant equal to that of bulk silicon and is tetragonally distorted in the surface normal direction by 0.06%. The lattice is slightly dilated in agreement with previous studies [8,9].

Returning now to the diffuse scattering patterns of Figure 3, the following microstructural picture is offered as a possible explanation. Domains of the crystalline sponge a few tens of nm in size are misoriented with respect to the main structure. As before, the fact that the diffraction pattern remains normal to an axis going through the origin of reciprocal space for both (004) and (224) diffraction is consistent with rigid rotation of the domains away from their original orientation. The width of the intensity distribution in Figure 3(a) along K[hh0] suggests misorientations up to 0.7°. Since these domains are ≈ 10 nm in size or larger, a large lattice dilation is not expected, and the intensity remains centered about the substrate peak. Because the domains are rather large, this only explains the diffuse scattering for ΔK values within about 0.06 $Å^{-1}$ of the substrate peak (ΔK is distance in reciprocal space relative to the substrate reciprocal lattice point). Intensity at larger ΔK arises due to scattering from the randomly positioned, 2-5 nm diameter *voids* which permeate both the coherent, and the misoriented, sponge-like domains.

As a final example of reciprocal space analysis, Figure 4 shows results for (004) and (224) diffraction from a 0.013 Ω-cm, n-type sample, produced by anodization at 60 ma/cm^2 for 30 minutes. The sample is 95 µm thick and has a porosity of 48%. Here, diffraction and PL results were collected after the sample was stored in air for three days. For both the n^+ and p^+ material we examined, there was always an intense coherent diffraction peak located near the substrate

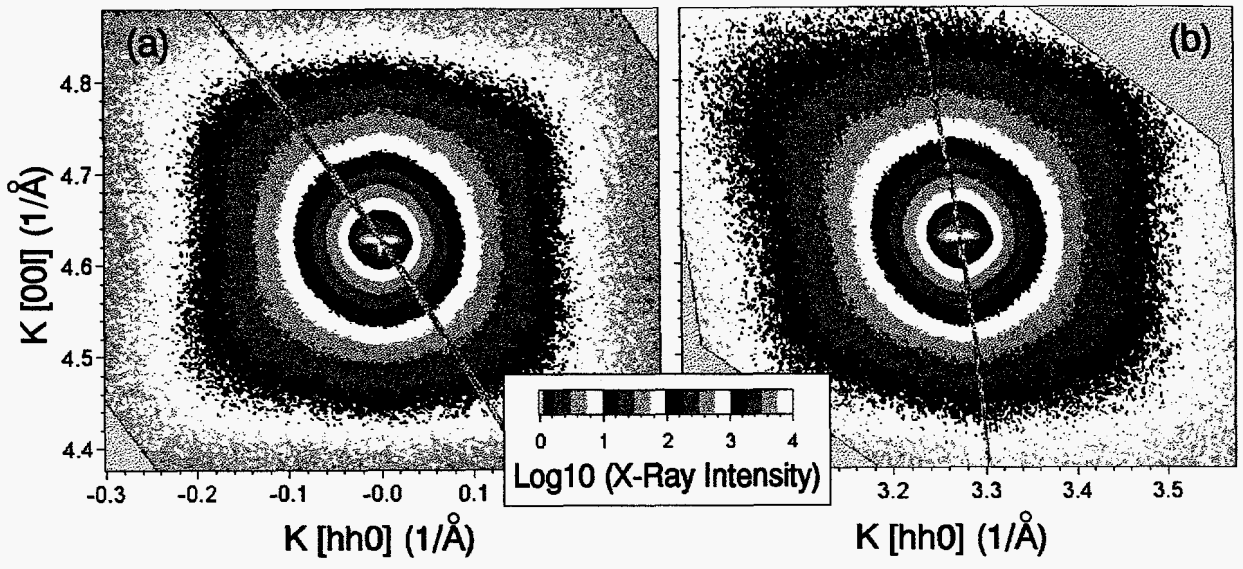

Figure 4. (a) the (004) diffraction pattern, and (b) the (224) diffraction pattern produced by n^+ porous Si composed of a single crystal layer penetrated by an vertical array of pores. Diffraction from nanovoids adjacent to the main pores appear to explain these patterns.

diffraction peak, indicating that these materials are primarily slightly strained single-crystals. The dense array of vertical pores in these samples produces a crossbar of intensity centered on the strain peak. This crossbar is barely seen near the center of Figures 4(a) and (b). Bensaid et al. [10] provide both an explanation for the crossbar intensity based on correlated spacing of the pores and a brief discussion of diffraction by randomly positioned voids.

In Figure 4, diffraction from nm-sized domains is again observed. In contrast to the above p^- results, the diffraction pattern does not change its basic orientation when going from (004) to (224) diffraction. This indicates that misoriented domains are not the main source of diffracted intensity for this sample. Here, the shape of the intensity distribution along K[00l], and the symmetry of the diffraction pattern, suggests scattering from approximately spherical domains 2-20 nm in size. However, since embedded nano*crystals* are expected to exhibit both appreciable misorientations and dilations that are not seen in Figure 4, it is believed that this diffraction pattern may again result from diffraction by nano*voids*. TEM of similar n^+ samples shows a graded structure with pores in the upper region being surrounded by nm-sized domains [11].

PHOTOLUMINESCENCE RESULTS

Photoluminescence spectra for the above samples appear in Figure 5 as curves (a), (b) and (e) along with spectra for two other samples we are studying. The same collection efficiency and pump power was used for each sample so that the spectral intensities could be compared.

First we consider p^- samples which contained dilated nanocrystals. The most intense PL signal (curve (a)) came from the aged p^- sample anodized at 80 ma/cm^2 (presented first above). This spectrum also exhibits strong intensity oscillations not seen in the other samples. These oscillations could be eliminated by tilting the sample to an 85° incident beam angle, or by using the 514 nm Ar line for excitation. Curves (c) and (d) in Figure 5 are for p^- samples anodized under much different conditions, but which also PL near 690 nm. Sample (c) produces a very weak, almost undetectable, nanocrystal diffraction pattern while sample (d) has a clear, but weak, nanocrystal diffraction pattern. Yet, these samples have PL integrated intensities that are 37% and 17%, respectively, of the intensity of curve (a). Superficially, there appears to be a lack of correlation between relative nanocrystal density and PL intensity that does not support

the quantum confinement mechanism for PL emission. However, these three samples have substantial differences in thickness, porosity, and perhaps nanocrystal size, that have not yet been fully determined. An ongoing part of the present work is to take these factors into account in order to more carefully extract relative nanocrystal densities from the reciprocal space maps. Ultimately, a quantitative comparison of nanocrystal density and PL intensity will be made.

Next, the 4-day-old, p^- sample which was structurally analyzed second above, and which is believed to be a crystalline sponge with misoriented domains a few tens of nm in size, luminesced strongly, but was red-shifted to 760 nm (Figure 5(b)). This PL result does not appear to be explained by a quantum confinement mechanism *unless* quantum confinement effects can occur in an extended, sponge-like, single-crystal structure ten or more nm on a side that is made up of smaller nm-sized interconnections. A possible complicating factor here is that the diffraction pattern produced by nanovoids in the sponge-like domains could be masking weaker diffraction by nanocrystals, which may be present at a lower number density. Again a more quantitative approach appears needed.

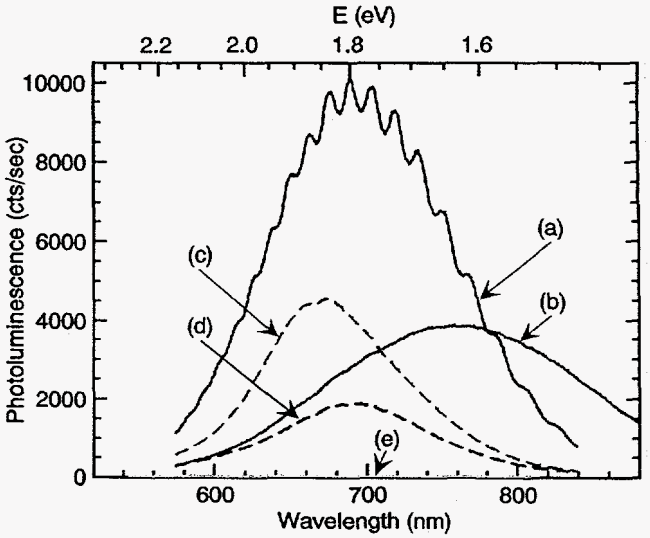

Figure 5. Photoluminescence spectra: (a) > 1-yr-old p^-, 80 ma/cm^2 in (1:1) HF:ethanol, (b) new p^-, 80 ma/cm^2 in (1:1) HF:ethanol, (c) > 1-yr-old p^-, 20 ma/cm^2 in (1:10) HF:H_2O, (d) new p^-, 10 ma/cm^2 in (1:10) HF:H_2O, (e) n^+ and p^+.

Finally, none of the n^+ or p^+ samples that were examined luminesced above background. Moreover, these samples did not appear to contain dilated nanocrystals in the few-nm-size range.

REFERENCES and ACKNOWLEDGMENTS

This work was supported by the U.S. Department of Energy under contract DE-AC04-94AL85000 and was partially funded by the Sandia National Laboratories LDRD program.

[1] T.R. Guilinger, M.J. Kelly, J.O. Stevenson, A.J. Howard, J.E. Houston and S.S. Tsao, in Proceedings of the Electrochemical Microfabrication Symposium, The Electrochemical Society, Phoenix, AZ, Oct. 13-18, 1991.

[2] L.R. Thompson, G.J. Collins, B.L. Doyle and J.A. Knapp, J. Appl. Phys. **70**, 4760 (1991).

[3] S.T. Picraux, B.L. Doyle and J.Y. Tsao, in Semiconductors and Semimetals **33**, edited by T.P. Pearsall (Academic Press, Boston, 1991), pp. 139-220.

[4] S.R. Lee, B.L. Doyle, T.J. Drummond, J.W. Medernach and R.P. Schneider, Jr., to be published in Advances in X-Ray Analysis **38**, Proceedings of the 43rd Annual Conference on Applications of X-Ray Analysis, Steamboat Springs, CO, August 1-5, 1994.

[5] B. E. Warren, X-Ray Diffraction, (Addison-Wesley, Reading, MA, 1969) , pp. 27-30.

[6] M. Hamasaki, T. Adachi, S. Wakayama and M. Kikuchi, J. Appl. Phys. **49**, 3987 (1978).

[7] S. Veprek, Z. Iqbal, H.R. Oswald, F.-A. Sarott, J.J. Wagner and A.P. Webb, Solid State Commun. **39**, 509 (1981).

[8] K. Barla, R. Hérino, G. Bomchil and J.C. Pfister, J. Cryst. Growth **68**, 727 (1984).

[9] I.M. Young, M.I.J. Beale and J.D. Benjamin, Appl. Phys. Lett. **46**, 1133 (1985).

[10] A. Bensaid, G. Patrat, M. Brunel, F. de Bergevin and R. Hérino, Solid State Commun. **79**, 923 (1991).

[11] J.W. Medernach and T.J. Headley (private communication).